

OBN up/down-going wavefields separation in dual-tree complex wavelet domain

Zhang * Libin, Wang Wei, Zou Zhen, Li Yifan, Chen Zhigang and Wang Kebin, BGP, CNPC

Summary

In the processing of ocean bottom node (OBN) data, separation of up-going and down-going wavefields through combination of the hydrophones pressure component (P) and geophones vertical component (Z) is useful for receiver side deghosting through P/Z summation and improving shallow image resolution through mirror migration. Precise matching of geophones to hydrophones is crucial for this method to work effectively. Additionally, the presence of scattered shear noise in the Z component data is another major obstacle. In this paper, we propose a new approach that can achieve P/Z matching and shear noise attenuation simultaneously by local attribute matching with phase correction in the dual-tree complex wavelet transform (DTCWT) domain. Synthetic and real dataset examples verify the effectiveness of this method.

Introduction

In ocean bottom surveys, hydrophones are used to record the pressure wavefields and geophones are used to record the 3-components elastic wavefields. Due to the directional characteristics of the geophone and omnidirectional response of the hydrophone, the ghost wavefields recorded by hydrophones and geophones show reverse polarity while up-going wavefields share the same polarity. The hydrophones pressure (P) data and geophones vertical component (Z) data can thus be combined to attenuate the receiver-side ghosts and separate up-going and down-going wavefields (Barr and Sanders, 1989). However, There are two main challenges exist in wavefield separation. First is the P/Z matching. Additional calibration of geophones to hydrophones is needed so as to compensate for the differences in sensitivity and coupling. The second challenge is the presence of scattered shear wave noise in geophone data. The noise becomes more prevalent when the surrounding ocean bottom is complex. Since shear waves do not propagate in water, P data recorded by hydrophones is not contaminated by this kind of noise.

Presented geophone calibration methods can be roughly classified in two categories. The first kind of methods are based on the minimization of up-going energy in the down-going wave-field just above the ocean bottom (Schalkwijk et al. 1999). It is often challenging to apply these methods when the down-going ghosts and up-going multiples arrival

at about the same time or in the shallow water case that the primary and ghost arrival overlapping. The second kind of methods are based on cross-ghosting (Ball and Corrigan 1996). Because of the flat-seabed assumption, these methods have difficulty in dealing with data from areas with rough seabed structure.

Shear wave noise attenuation methods have been proposed. Based on a 1-D approximation for the velocity model of water layer, the noise can be simulated and the signal can be separated (Brittan and Starr 2003). The requirement for a 1-D velocity model is hardly suited for complex seafloors and subsurface structures. F-K domain velocity filtering can be used for shear wave attenuation (Shatilo et al. 2004). Both signal and shear wave noise appearing in a very large range of dipping angles caused by complex geologies is an obstacle for this method.

P/Z matching and shear wave noise attenuation can be achieved in one step with local attribute matching in the dual-tree complex wavelet transform (DTCWT) domain (Yu, et al. 2011). This method can improve both the efficiency and quality of the up/down-going wavefields separation. In this paper, we further develop this method with an additional phase correction that can improve the effect of up/down-going wavefields separation.

Method

The dual-tree complex wavelet transform (DTCWT) is a relatively enhancement to the discrete wavelet transform (DWT) with additional properties of nearly shift invariant and directional selectiveness (Kinsbury 2001). Using complex-valued filtering, DTCWT can decomposes real signals into multi-resolution and multi-directionality real and imaginary parts. Moreover, the real and imaginary coefficients satisfy the Hilbert relation and can be used to compute amplitude and phase information (Yu, et al. 2011). 2D DTCWT of a 2D input data $d(t, x)$ can be represented:

$$D(t, x, s, o, ri) = DTCWT[d(t, x)]$$

Where D is the 2D DTCWT coefficient array, in which t and x are time and spatial coordinate vectors respectively; s is a scale vector representing resolution as show in the columns of Figure 1; o is an orientation vector containing 6 elements ($\pm 75, \pm 45, \pm 15$ degree) at each scale as shown in the rows of Figure 1; ri is a real part vector and an imaginary part vector.

OBN up/down-going wavefields separation in dual-tree complex wavelet domain

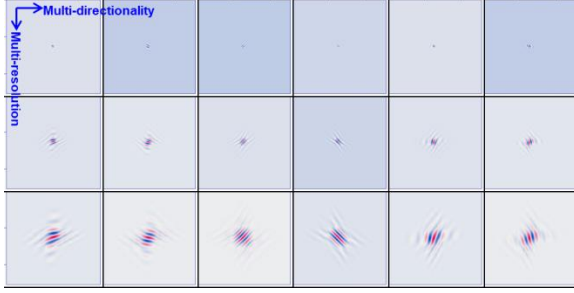


Figure 1: Point pulse response of 2D DTCWT. Orientations in the rows from left to right are +/-15, +/-45 and +/-75 degree respectively. Scales in the columns from top to bottom are 1, 2, 3 respectively.

Since the hydrophone data (P) is free of shear wave noise, geophone vertical particle data (Z) can be matched to P according to their local attributes in the DTCWT domain to achieve P/Z matching and shear noise attenuation simultaneously. Differing from the method presented by Yu, et al. (2011) that matches P/Z envelopes only and preserves their phases unchanged, our method matches the envelopes and implements phase correction to improve the effect of wavefields separation. We take the phase difference between P and Z as an indicator to recognize effective signals and noises including the receiver-side ghosts and the scattered shear energy. When the phase difference is less than a certain low threshold, the corresponding P/Z data is considered as signals and Z is matched to P with both the same envelopes and phases. When the phase difference is greater than a certain high threshold, the corresponding P/Z data is considered as noises and Z is matched to P with the same envelopes and reverse phases. When the phase difference falls between a certain low threshold and a certain high threshold, Z is matched to P with the same envelopes only and preserves its original phases unchanged. Our matching operation can be defined as:

$$\begin{cases} ZT'(t, x, s, o, ri) = PT(t, x, s, o, ri) & dPH < Threshold_{low} \\ ZT'(t, x, s, o, ri) = ZT(t, x, s, o, ri) * |PT|/|ZT| & Threshold_{low} \leq dPH \leq Threshold_{high} \\ ZT'(t, x, s, o, ri) = PT(t, x, s, o, -ri) & dPH > Threshold_{high} \end{cases}$$

Where $PT(t, x, s, o, ri)$ is the forward 2D DTCWT of hydrophone data $P(t, x)$; $ZT(t, x, s, o, ri)$ is the forward 2D DTCWT of geophone vertical particle data $Z(t, x)$; $ZT'(t, x, s, o, ri)$ is the matched version of $ZT(t, x, s, o, ri)$; and

$$|PT| = \sqrt{PT(t, x, s, o, r)^2 + PT(t, x, s, o, i)^2}$$

$$|ZT| = \sqrt{ZT(t, x, s, o, r)^2 + ZT(t, x, s, o, i)^2}$$

$$dPH = \left| \arctan\left(\frac{PT(t, x, s, o, i)}{PT(t, x, s, o, r)}\right) - \arctan\left(\frac{ZT(t, x, s, o, i)}{ZT(t, x, s, o, r)}\right) \right|$$

$|PT|$ is the amplitudes of $PT(t, x, s, o, ri)$; $|ZT|$ is the amplitudes of $ZT(t, x, s, o, ri)$; dPH is the phase difference between $PT(t, x, s, o, ri)$ and $ZT(t, x, s, o, ri)$; $Threshold_{low}$ is a certain low threshold of dPH ; $Threshold_{high}$ is a certain high threshold of dPH .

The up/down-going wavefields separation workflow (Figure 2) proposed in this paper mainly includes the following steps: (1) 2D forward DTCWT of both hydrophone data (P) and geophone vertical particle data (Z), (2) Matching Z coefficients to P coefficients in the 2D DTCWT domain with the operator presented above, (3) 2D inverse DTCWT of the matched Z-component coefficients, and (4) combining the hydrophone data (P) and matched geophone vertical particle data (Z) in the original time and spatial domain to separate the up-going and down-going wavefields.

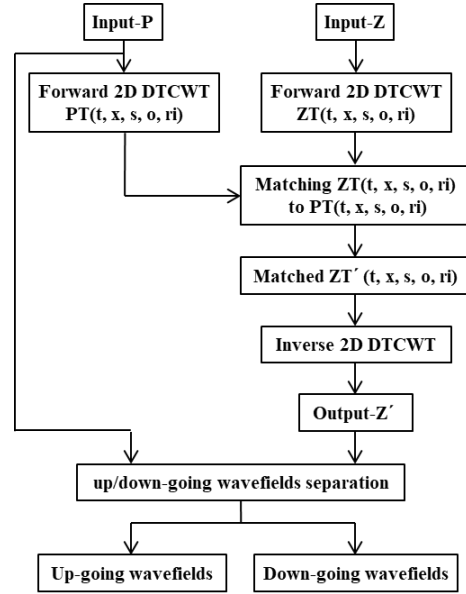


Figure 2: The presented up/down-going wavefields separation workflow.

Examples

To verify the effectiveness of our method, we generated a synthetic OBN survey with P and Z records as shown in Figure 4. The velocity mode used to generate the synthetic data is shown in Figure 3. Fig 4-a is P data and Fig 4-b is Z data. The red triangle in Figure 3 marks the position where they are recorded. It is obvious that there are strong ghosts in Fig 4-a marked area and apparent primary in Fig 4-b marked area. Figure 5 is the wavefields separation results achieved by cross-ghosting method. Fig 5-a is the up-going wavefields. Fig 5-b is the down-going wavefields. Figure 6 is the wavefields separation results achieved by DTCWT method without phase correction. Fig 6-a is the up-going wavefields and Fig 6-b is the down-going wavefields. Figure 7 show the wavefields separation results achieved by DTCWT method with phase correction. Fig 7-a is the up-going wavefields. Fig 7-b is the down-going wavefields.

OBN up/down-going wavefields separation in dual-tree complex wavelet domain

Comparing these separated up-going and down-going wavefields, DTCWT methods is better than cross-ghosting method and DTCWT method with phase correction is significantly better than DTCWT method without phase correction.

A field OBN data wavefields separation test has been shown in Figure 8 to Figure 10. In Figure 8, Fig 8-a is the P data and Fig 8-b is the Z data. Heavy shear wave noise can be seen in the Z record in the marked area. Figure 9 is the wavefields separation results achieved by DTCWT method with phase correction. Fig 9-a is the up-going wavefields. Fig 9-b is the down-going wavefields. The shear wave noise has been attenuated significantly and hardly been seen in both of the up-going wavefields and the down-going wavefields. The field data stacking sections are shown in Figure 10. Fig 10-a is the P component wavefields stacking section. Fig 10-b is the Z component wavefields stacking section. Fig 10-c is the up-going wavefields stacking section achieved by cross-ghosting method. Fig 10-d is the up-going wavefields stacking section achieved by DTCWT method with phase correction. We can see that the section shown in Fig 10-d is much better than the section shown in Fig 10-c especially in the marked low S/N ratio area. It verifies the denoising superiority of DTCWT method presented in this paper.

Conclusions

We have proposed a new DTCWT method with phase correction for ocean bottom seismic data shear wave attenuation and up/down-going wavefields separation. It can calibrate the geophone data with the hydrophone data and suppress shear wave noise simultaneously in the DTCWT domain, which improves both the effectiveness and efficiency of the wavefields separation. The synthetic and field dataset examples verify the effectiveness of this method.

Acknowledgments

The authors thank BGP for the permission to publish this work. This work is financially supported by CNPC Scientific Research and Technology Development Project (No. 2021ZG02, Development of ocean bottom node (OBN) seismic data processing software).

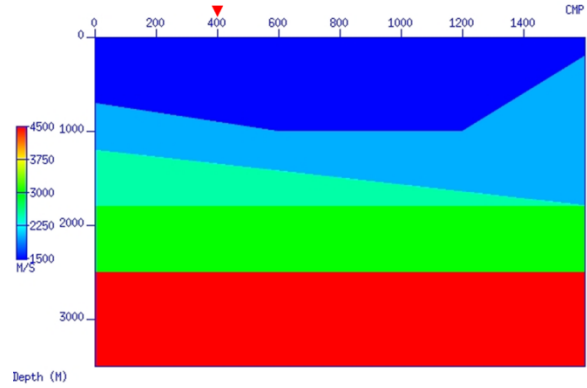


Figure 3: Velocity mode used to generate synthetic OBN records.

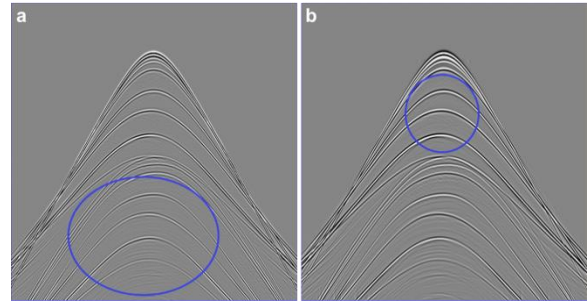


Figure 4: Synthetic OBN records. Fig 4-a is P data and Fig 4-b is Z data.

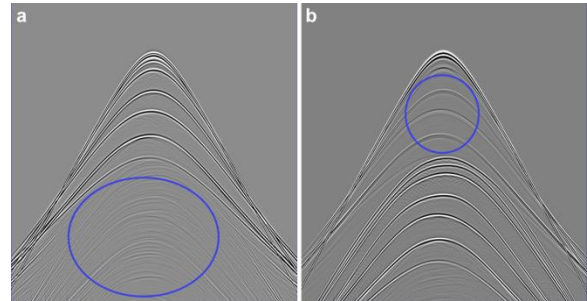


Figure 5: Wavefields separation results achieved by cross-ghosting method. Fig 5-a is the up-going wavefields. Fig 5-b is the down-going wavefields.

OBN up/down-going wavefields separation in dual-tree complex wavelet domain

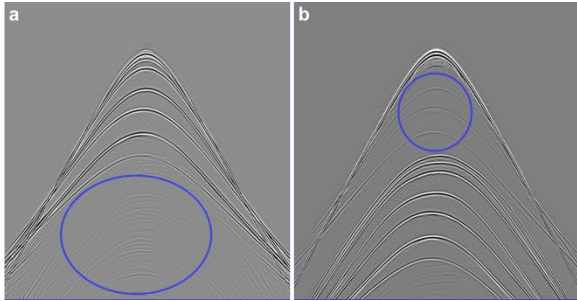


Figure 6: Wavefields separation results achieved by DTCWT method without phase correction. Fig 6-a is the up-going wavefields. Fig 6-b is the down-going wavefields.

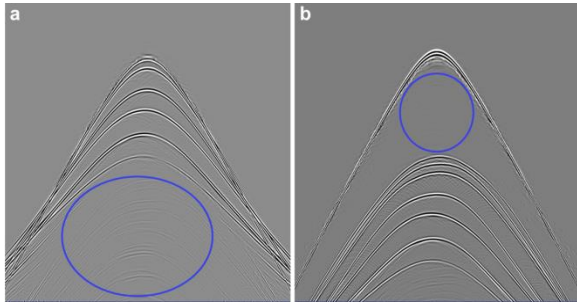


Figure 7: Wavefields separation results achieved by DTCWT method with phase correction. Fig 7-a is the up-going wavefields. Fig 7-b is the down-going wavefields.

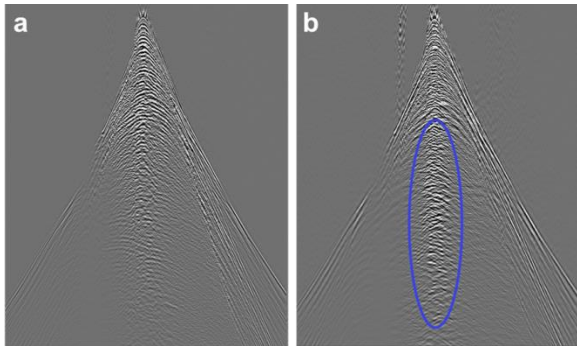


Figure 8: Field OBN records. Fig 8-a is the P data and Fig 8-b is the Z data.

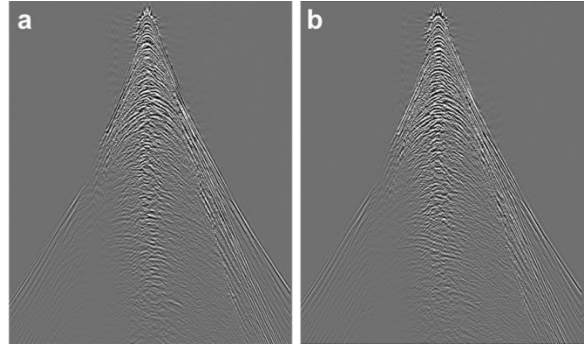


Figure 9: Wavefields separation results achieved by DTCWT method with phase correction. Fig 9-a is the up-going wavefields. Fig 9-b is the down-going wavefields.

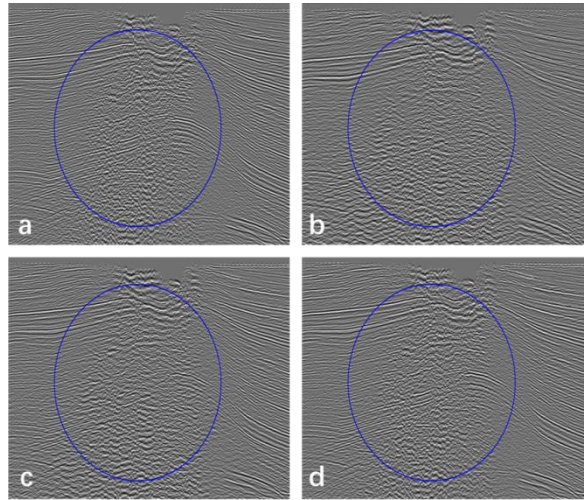


Figure 10: Field data stacking sections. Fig 10-a is the P component wavefields stacking section. Fig 10-b is the Z component wavefields stacking section. Fig 10-c is the up-going wavefields stacking section achieved by cross-ghosting method. Fig 10-d is the up-going wavefields stacking section achieved by DTCWT method with phase correction.